

~~SECRET~~
~~SECURITY INFORMATION~~

428
R.F

INVENTORY 1958

MARTIN MARIETTA ENERGY SYSTEMS LIBRARIES



3 4456 0360903 0

ORNL-1133, Part 2
Preliminary Draft

19A



REC RESEARCH AND DEVELOPMENT REPORT



THE SHIELDING OF MOBILE REACTORS - II

DECLASSIFIED

CLASSIFICATION CHANGED TO:

BY AUTHORITY OF: TID-1219
BY: M. Tallest 3/29/60



OAK RIDGE NATIONAL LABORATORY
CENTRAL RESEARCH LIBRARY
CIRCULATION SECTION
4500N ROOM 175
LIBRARY LOAN COPY
DO NOT TRANSFER TO ANOTHER PERSON
If you wish someone else to see this report, send in name with report and the library will arrange a loan.

UCN-7969 (3 9-77)

OAK RIDGE NATIONAL LABORATORY
OPERATED BY
CARBIDE AND CARBON CHEMICALS COMPANY
A DIVISION OF UNION CARBIDE AND CARBON CORPORATION



POST OFFICE BOX P
OAK RIDGE, TENNESSEE

~~SECRET~~
~~SECURITY INFORMATION~~

[REDACTED]

ORNL 1133, Part 2
Preliminary Draft

(This is a draft of an article to appear
in the REACTOR SCIENCE AND TECHNOLOGY)

This document consists of 55
pages. No. 19 of 170 copies,
Series A.

Contract No. W-7405, eng 26

PHYSICS DIVISION

THE SHIELDING OF MOBILE REACTORS - II

E. P. Blizard and T. A. Welton

Date Issued:

OAK RIDGE NATIONAL LABORATORY
operated by
CARBIDE AND CARBON CHEMICALS COMPANY
A Division of Union Carbide and Carbon Corporation
Post Office Box P
Oak Ridge, Tennessee

UNCLASSIFIED DATA

This document is classified as [REDACTED] defined
in the [REDACTED]
of the [REDACTED]
[REDACTED]

[REDACTED]

~~SECRET
SECURITY INFORMATION~~

ORNL 1133 - Part 2
Preliminary Draft

~~INTERNAL DISTRIBUTION~~

1. E. E. Blizard
2. R. C. Briant
3. C. E. Clifford
4. H. L. F. Enlow
5. A. P. Fraas
6. F. K. McGowan
7. J. L. Neep
8. F. J. Szenthaler
9. F. H. Murray
10. J. D. Fenn
11. T. V. Kasser
12. H. E. Sniderford
13. R. G. Lockman
14. E. B. Johnson
15. G. T. Chapman
16. R. Ritchie
17. A. Salmon
18. A. Snell
19. M. Weinberg
20. A. Welton
21. O. Wollan
22. Physics Library
- 23-43 Central Files
- 43-17 Central Files (O.P.)

~~RESTRICTED~~
contains restricted data as defined
the Atomic Energy Act of 1946. Its transmittal
or the disclosure of its contents to

~~-ii-~~

~~[REDACTED]~~



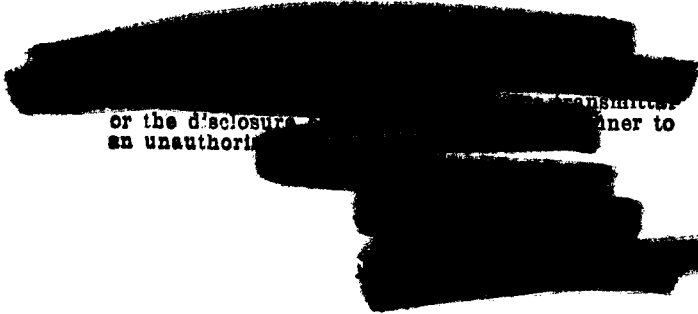
3 4456 0360903 0



ABSTRACT

The methods of applying results of bulk shielding measurements to the design of reactor shields is outlined. Geometrical transformations for the more common shapes are derived, as are approximate means of calculating leakage of radiation.

As an illustration of the methods, the ORNL Lid Tank and Bulk Shielding Facility data are transformed to a standard geometry and compared. Two direct calculations of water attenuation, using cross sections described in the previous article, are finally compared with the experimental data.



or the disclosure of the transmitter
an unauthorized person to



THE SHIELDING OF MOBILE REACTORS - II

E. P. Blizard and T. A. Welton*

INTRODUCTION

Up to the present time it has been impossible to design a reactor shield solely on the basis of measured cross sections. The large attenuations which are required make the multiply-scattered radiation dominant, so that a direct calculation not only becomes excessively complicated, but also is dependent upon a much more complete knowledge of differential cross sections than is presently available.

As a consequence, shield design is based entirely on large-scale attenuation experiments, the data from which can be used in either of two ways. In the so-called "comparison method" the geometry of the experiment is transformed to that of the reactor to be shielded, and source strengths and dose rates are appropriately adjusted. The phenomenological approach is adhered to as much as possible, using power and dose rates as the observables and relying on knowledge of the attenuation processes only to a very limited extent.

In the direct calculation method, on the other hand, the shielding experiments are used to determine "effective removal cross sections"¹ for the elements of the shield, and from these the attenuation is determined by simple calculation. As was pointed out in the previous article, the effective removal cross

*Note: Neither author is senior to the other.





sections are by definition those which make simple exponential attenuation apply. This method has been limited for neutrons to shields which are mostly water with a small volume percentage of iron or lead. Since the constituents of water have not been measured separately, the whole cross section of hydrogen is used, and the effect of the oxygen is inferred from the experiments.

Of the two, certainly the comparison method is more reliable and more generally applicable. For shields which are primarily water, however, the direct approach is often convenient for the calculation of neutron attenuation.

Gamma attenuation in the absence of neutrons has been well treated in other papers and need not be repeated here.²⁻⁵ Only very little theoretical work has been done, however, on gamma intensity at the outside of a reactor shield in which the neutrons constitute a sizeable secondary source. Since this case is a very important one in many mobile shields, it is fortunate that the comparison method applies, although it must be ascertained whether the gamma rays which emerge from the shield are produced within the shield or the reactive core.

The present article will first describe the Lid Tank Shielding Facility, give the more common geometrical transformations, including a method for comparison of source strengths, and then demonstrate the comparison method of shield design by computing the water shielding for the Bulk Shielding Reactor (BSR). Next neutron attenuation in water will be calculated using the hydrogen cross section derived in the previous article and adjusting the oxygen cross section to fit the



Lid Tank data. From this analysis another prediction will be made of the fast-neutron dose in the water surrounding the BSR. An additional calculation including ageing will estimate the thermal flux. These calculations will then be compared with the measurements as taken at Oak Ridge.

THE LID TANK SHIELDING FACILITY⁶

The Oak Ridge graphite reactor was originally designed so that the central core of graphite could be removed en masse through a "core removal hole" in the shield of the west, or discharge, face of the pile. A special well-reinforced balcony was built to hold the core plus a lead shield. Although neither the hole nor the balcony was ever used as originally intended, both served excellently as the basis for a shield-testing facility. Over the shield hole, which is 28 by 32 in. at the outside, is placed a closely packed flat array of natural uranium cylinders which is irradiated by thermal neutrons from the pile. Some of the fast neutrons and gamma rays that result then enter a large water tank which is mounted over the "source plate," being attenuated by the water or whatever shield is placed in the tank.

Figure 1 is a photograph taken from above the Lid Tank showing some of the apparatus for radiation detection. Figure 2 shows the location of the source with respect to the tank, and Figure 3 shows the structure of the source plate.

The source plate is made effectively a 28-in. diameter disc by a fixed

~~SECRET~~

iris of B_4C painted on thin aluminum which shields the uranium from thermal neutrons except within this circle. A shutter, also of B_4C on aluminum, can be moved across the core hole mouth at the outside to cut off the beam of thermal neutrons, thus permitting background measurements. An isolation curtain of B_4C on aluminum is permanently installed between source plate and water tank to insure that back-scattering of neutrons from the tank or its contents will not alter the fission rate unexpectedly.

The source power was measured by observing the temperature of the uranium as a function of time after opening or closing the shutter. The value so obtained was 6 watts for the total effective area of 3970 cm^2 .

GEOMETRICAL TRANSFORMATIONS

Type of Detector

For collimated radiation in free space the directional dependence of the detector need not be known, provided of course that its sensitivity for the prime direction is given. When, however, radiation arises from many directions, this ambiguity is no longer tolerable. Accordingly the two types of most use are now defined. It should be pointed out that the detectors to be described are not those which might be used in an experiment, but rather hypothetical pure types for which calculations can be made. Most actual detectors, including the human body, resemble both types to some extent, but usually one more than the other.

~~SECRET~~

~~SECRET~~

Directional Detector. This detector can be characterized by a small flat black body which records the total number or intensity of arrivals on its surface and is, unless otherwise specified, assumed to be perpendicular to the preferred direction of propagation. Thus the response is proportional to the cosine of the angle between actual arrival and the preferred direction. It is this type of detector which is to be used in calculating the total leakage from a surface, or the total arrivals at a surface, either of which could be used to specify a second source, say due to neutron captures. It is approached experimentally by a foil so thick that essentially all incident neutrons record. The reading on this detector will in general be indicated by J, implying a radiation current.

Isotropic Detector. The isotropic detector is characterized by a small black sphere, which of course presents the same target size to all directions. This detector is sometimes referred to as a "milligoat" since a small meatball would presumably serve as a useful detector if the dosage in it could be recorded. It is obvious that this detector will always record an intensity of radiation at least as high as that recorded on the directional detector, and hence the milligoat reading gives the maximum rate of radiation reception by, for example, the human body. It should be used, therefore, whenever the radiation is not definitely collimated. It can always be used for an upper limit, which gives of course a conservative shield design. The response of this detector will in general be indicated by D, implying a dose rate. The area by which the rate of

~~SECRET~~

~~CONFIDENTIAL~~

arrivals must be divided to obtain flux is that of a great circle of the sphere (radius = $1/\sqrt{\pi}$).

General Transformations for Unspecified Attenuation Functions

In shielding theories, attenuation is usually expressed in terms of either a point source or an infinite plane collimated source in an infinite medium. Most shielding measurements have been made with a uniform disc source in a "semi-infinite" medium. Most reactors, on the other hand, approximate cubes, cylinders, or spheres. In order to convert from one shape to another certain geometrical manipulations are used which will presently be demonstrated.

The Point-to-Point Attenuation Kernel. For the purpose of calculating the intensity in other geometries, a function $G(R)$ is used, which is defined as the response of a detector at a distance R in the shield from a unit source. $G(R)$ is of course characteristic of the source, the detector, and the medium. Thus the source might be a gamma emitter, the medium water, and the detector an ionization chamber. The source must be isotropic, the detector non-directional, and the medium must attenuate the same for all distances R regardless of position or direction. Thus, for a point source of strength S a distance R from an isotropic detector,

$$D_{\text{Pt.}}(R) = S G(R). \quad (1)$$

~~SECRET~~

Of course the conditions imposed on $G(R)$ are never exactly satisfied in experiment or installation, but usually, on the other hand, it is a good approximation to use the results derived with the aid of the ideal functions. Some of the conditions which make $G(R)$ not a unique function of R are the following:

a. The source itself is not infinitely small or thin and consequently absorbs some of its own radiation, leaving the remainder not isotropic. This absorption is not always comparable to that of the shield material displaced.

b. The "medium" seldom is present on both sides of a plane source, as is required in the assumption.

c. Not only does the medium terminate before infinite -- it usually cuts off just at the measuring point so that the effect may in some cases be appreciable.

d. Many shields are laminated so that the properties of the medium are not isotropic, that is, they do not attenuate at the same rate for all directions. This can be especially true for gamma rays.

e. Reactors are of considerable size, hence are often treated as if the surface were a thin isotropic source and the volume is counted as shielding medium. Both assumptions are obviously incorrect, but the inaccuracies they introduce are usually not excessive. Treatment of reactor material as if it were

~~SECRET~~

~~SECRET~~

shielding is not a bad approximation, since after all the purpose of most of the material is to "contain" the neutrons, i.e., to attenuate the fast neutrons.

Plane Isotropic Source in Infinite Medium. In this case the source is assumed infinitely thin, all in one plane, or of uniform strength σ particles emitted isotropically per unit area of source per unit time, and imbedded in an infinite uniform medium. The response of the isotropic detector at a distance z away from the infinite source, $D_{PI}(z, \infty)$, is now calculated:

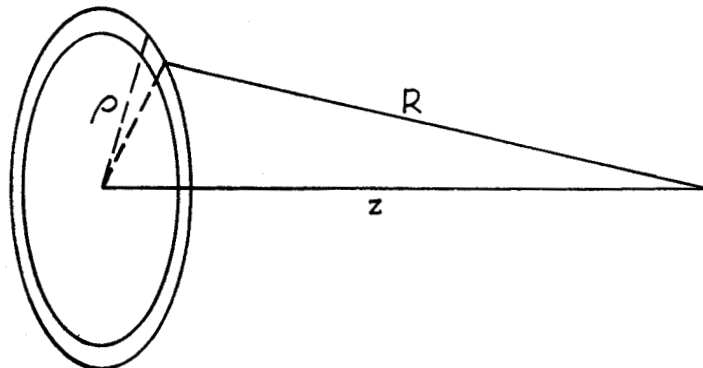


Fig. 4

$$D_{Pl}(z, \infty) = \int_{\rho=0}^{\infty} 2\pi\rho \, d\rho \, \sigma G(R)$$

$$R^2 = \rho^2 + z^2$$

$$2R \, dR = 2\rho \, d\rho$$

$$D_{Pl}(z, \infty) = 2\pi\sigma \int_z^{\infty} G(R) R \, dR. \quad (2)$$

The relation between point and plane source geometries is obtained by differentiating Eq. (2),

$$\frac{d}{dz} D_{Pl}(z, \infty) = -2\pi\sigma z G(z), \quad (3)$$

$$\frac{d}{dz} D_{Pl}(z, \infty) = -2\pi \frac{\sigma}{S} z D_{Pt}(z). \quad (3a)$$

In case the plane source is confined to a disc of radius "a" and the detector is on the axis of the source,

$$\begin{aligned} D_{Pl}(z, a) &= \int_{\rho=0}^{\rho=a} 2\pi\sigma\rho \, d\rho \, G(R) \\ &= 2\pi\sigma \int_z^{\sqrt{z^2 + a^2}} G(R) R \, dR. \end{aligned} \quad (4)$$

~~SECRET~~

Since much of the experimental work on shielding has been carried out with a disc source, it is important to investigate a method of obtaining more fundamental information from the observed data. That is, it is desirable to find the point-to-point kernel from data taken at points on the axis of a disc source. For this purpose, Eq.(4) is differentiated with respect to z .

Thus:

$$D'_{Pl}(z,a) = 2\pi\sigma \left[G(\sqrt{z^2+a^2}) \sqrt{z^2+a^2} \frac{d}{dz} \sqrt{z^2+a^2} - G(z) z \right]$$

$$\frac{D'_{Pl}(z,a)}{2\pi\sigma z} = G(\sqrt{z^2+a^2}) - G(z) \quad (5)$$

Defining $B(z) = - \frac{D'_{Pl}(z,a)}{2\pi\sigma z}$,

it is found, using the recursion formula (5), that

$$G(z) = B(z) + B(\sqrt{z^2+a^2}) + B(\sqrt{z^2+2a^2}) + \dots$$

$$= \sum_{\nu=0}^{\infty} B(\sqrt{z^2+\nu a^2}) \quad (6)$$

~~SECRET~~

The last equation defines a method of determining the kernel from the data using straightforward operations. It is only applicable for "a" large compared to the attenuation length of the radiation, but for those cases in which this condition is not met the disc will be a good approximation to a point source and the data will indicate $G(R)$ directly.

Plane to Sphere Transformation. It is often of interest to calculate the intensity to be expected from a source spread uniformly over the surface of a sphere. The usual isotropic medium is assumed, and this must extend inside as well as outside the sphere. The geometry is shown in Fig. 5.

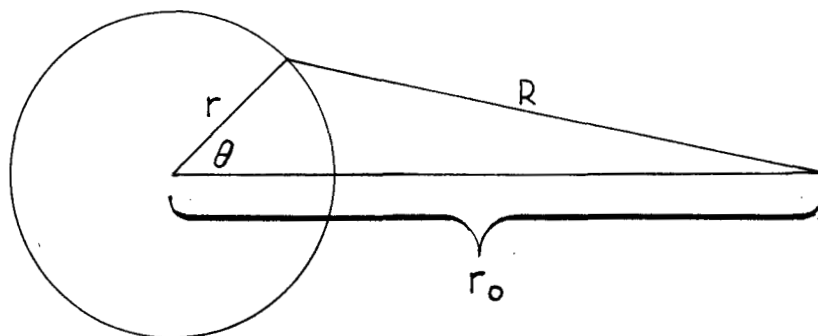


Fig. 5

For this case

$$D_S(r_0, r) = 2\pi\sigma r^2 \int_{\theta=0}^{\pi} G(R) \sin\theta \, d\theta,$$

$$R^2 = r^2 + r_0^2 - 2rr_0 \cos\theta ,$$

$$2R \, dR = 2rr_0 \sin\theta \, d\theta,$$

$$D_S(r_0, r) = 2\pi\sigma \frac{r}{r_0} \int_{r_0-r}^{r_0+r} G(R) R \, dR$$

$$= \frac{r}{r_0} \left\{ 2\pi\sigma \int_{r_0-r}^{\infty} G(R) R \, dR - 2\pi\sigma \int_{r_0+r}^{\infty} G(R) R \, dR \right\}$$

$$= \frac{r}{r_0} \left\{ D_{Pl}(r_0 - r, \infty) - D_{Pl}(r_0 + r, \infty) \right\} \quad (7)$$

If $2r \gg \lambda$, the relaxation length, then the second term in the bracket will be negligible compared to the first, and the following approximate expression becomes useful:

$$D_S(r_0, r) \approx \frac{r}{r_0} D_{Pl}(r_0 - r, \infty) \quad (8)$$

~~SECRET~~

Plane to Cylinder Transformation. There is no simple general transformation for this case, but it can be shown for most specific attenuation kernels that the relation between cylindrical and plane geometry for large attenuations (thick shields) should be approximately

$$D_C(r_0, r) \approx \sqrt{\frac{r}{r_0}} D_{P\lambda}(r_0 - r, \infty) , \quad (9)$$

where

$D_C(r_0, r)$ is the dose to be expected from an infinitely long cylindrical source of surface strength σ imbedded in shielding material,

r_0 is the distance from the axis to the measuring point,

r is the cylinder radius,

$D_{P\lambda}(r_0 - r, \infty)$ is the dose to be expected at a distance $r_0 - r$ from an infinite plane source of surface strength σ , imbedded in the same shielding material.

This relation (9) is not unreasonable, in that the cylinder is intermediate between plane and sphere, and the factor of proportionality, $\sqrt{r/r_0}$, is intermediate between unity and that for plane to sphere, Eq. (8).

~~SECRET~~

~~CONFIDENTIAL~~

Although it is possible to extend the treatment of transformations somewhat further without specifying the form of the attenuation kernel, nevertheless it is usually much easier to choose some simple form which will fit at least over a limited range and to use this in the transformations. The next section demonstrates this method.

Geometry for Partially Specified Attenuation Functions

In this section advantage will be taken of the fact that the attenuation in shields is large, so that contributions from the nearest sources are dominant and crude approximations are adequate to indicate the additional contributions of more distant sources. This process is commonly used in shielding with considerable success.

Consider an isotropic source spread uniformly over a curving surface so that the strength of the source on an element of area dS is just σdS . Let the nearest source point be located at the origin, the surface being tangent to the xy plane at the origin and then curving away so that the distance between the surface and the xy plane is given approximately by

$$z_1 = \frac{1}{2} \left(\frac{x^2}{a} + \frac{y^2}{b} \right). \quad (10)$$

Thus "a" and "b" are the normal curvatures of the surface, and use of Eq.(10) is a direct consequence of the assumption regarding distant sources, since it

~~CONFIDENTIAL~~

surely will not fit well except in the region near the origin.

The detector is at z , and the distance from this to the element of surface dS is R .

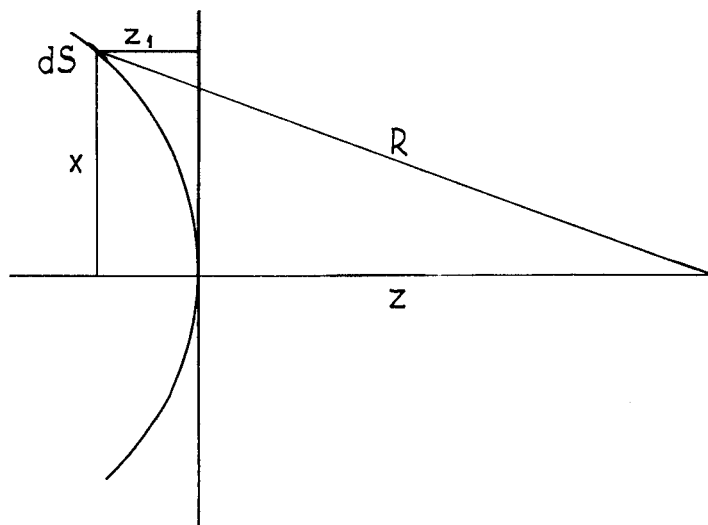


Fig. 6

The reading on a milligoat detector is then

$$D(z) = \sigma \int_{\text{Surface}} G(R) dS, \quad (11)$$

$$dS = dx dy \sqrt{1 + \left(\frac{\partial z_1}{\partial x}\right)^2 + \left(\frac{\partial z_1}{\partial y}\right)^2}$$

$$\approx dx dy \left(1 + \frac{x^2}{2a^2} + \frac{y^2}{2b^2}\right) \quad (12)$$

~~SECRET~~

G(R) is now approximated by an unspecified (and therefore presumably exact) function for the kernel for the distance z, times an exponential for the extra distance (R - z).

$$G(R) \approx G(z) e^{-(R-z)/\lambda} \quad (13)$$

λ is a relaxation length, presumably one which makes Eq. (13) correct. Actually, since λ will be slowly varying, it can be taken from almost any convenient data for the proper material and source with attenuation over a distance of about z. For example, λ could be taken directly from Lid Tank data.

An approximate form is now required for R in order to make Eq. (11) integrable,

$$R = \sqrt{(z_1 + z)^2 + x^2 + y^2} \quad (14)$$

On expanding and ignoring terms of the order of z_1^2 , in comparison with x^2 and y^2 , it is found that

$$R - z \approx \frac{x^2}{2z} + \frac{y^2}{2z} + \frac{x^2}{2a} + \frac{y^2}{2b} \quad (15)$$

If Eq. (15) is accepted as adequate,

$$D(z) = \sigma G(z) \int_{-\infty}^{\infty} dy \int_{-\infty}^{\infty} dx e^{-\frac{x^2+y^2}{2\lambda z} - \frac{x^2}{2\lambda a} - \frac{y^2}{2\lambda b}} \left[1 + \frac{x^2}{2a^2} + \frac{y^2}{2b^2} \right] \quad (16)$$

A cumbersome but not difficult integration yields

$$D(z) \approx 2\pi\sigma G(z) \left\{ \frac{1}{\left(\frac{1}{\lambda z} + \frac{1}{\lambda a}\right)^{\frac{1}{2}} \left(\frac{1}{\lambda z} + \frac{1}{\lambda b}\right)^{\frac{1}{2}}} + \frac{1}{2a^2 \left(\frac{1}{\lambda z} + \frac{1}{\lambda a}\right)^{\frac{3}{2}} \left(\frac{1}{\lambda z} + \frac{1}{\lambda b}\right)^{\frac{1}{2}}} \right. \\ \left. + \frac{1}{2b^2 \left(\frac{1}{\lambda z} + \frac{1}{\lambda a}\right)^{\frac{1}{2}} \left(\frac{1}{\lambda z} + \frac{1}{\lambda b}\right)^{\frac{3}{2}}} \right\} \quad (17)$$

The last two quantities in the braces are in general much smaller than the first for a and b large compared to λ .

$$D(z) \approx 2\pi\sigma G(z) \left[\frac{1}{\left(\frac{1}{\lambda z} + \frac{1}{\lambda a}\right)^{\frac{1}{2}} \left(\frac{1}{\lambda z} + \frac{1}{\lambda b}\right)^{\frac{1}{2}}} \right] \quad (18)$$

for $a, b \gg \lambda$.

For a sphere $a = b = r$,

$$z = r_0 - r$$

$$D_S(r_0, r) = 2\pi\sigma G(z) \lambda z \frac{r}{r_0} \quad (19)$$

██████████
██

If at this point it is recognized that

$$\frac{d}{dz} D_{P\ell}(z, \infty) = \frac{D_{P\ell}(z, \infty)}{\lambda}, \quad (20)$$

then it is possible at once to confirm that Eqs. (19) and (3) agree.

For a cylinder, $a = \infty$, $b = r$, and $z = r_0 - r$. By similar manipulation it is seen that Eq. (18) then confirms Eq. (9).

Comparison of Source Strengths

In order to compare the source which is used in a shielding experiment with that of an actual reactor, it is necessary to make some sort of estimate of the self-absorption in the two cases. Fortunately most of the radiation which leaks does so from the region near its periphery, so that it is quite adequate to calculate leakages using simple exponential attenuation. The core relaxation length can be either the mean free path or some better estimate based on comparison of cross sections and measured relaxation lengths. The section on effective removal cross sections, (I), described the latter. For the present a core relaxation length, λ_c , will be used for the attenuation in the reactive volume without specifying its origin.

It will be shown that to adequate accuracy the volume-distributed source can be replaced by a surface-distributed source which will give the same attenuated dose at the shield exterior. The relationship between the volume and surface

██████████
██

source strengths will also be derived for two common power distributions.

Consider a small volume, dv , of the reactor, the rate of power dissipation therein being $p(x,y,z)dv$. The total of contributions of elements such as this to the dose at some observation point outside the shield is required.

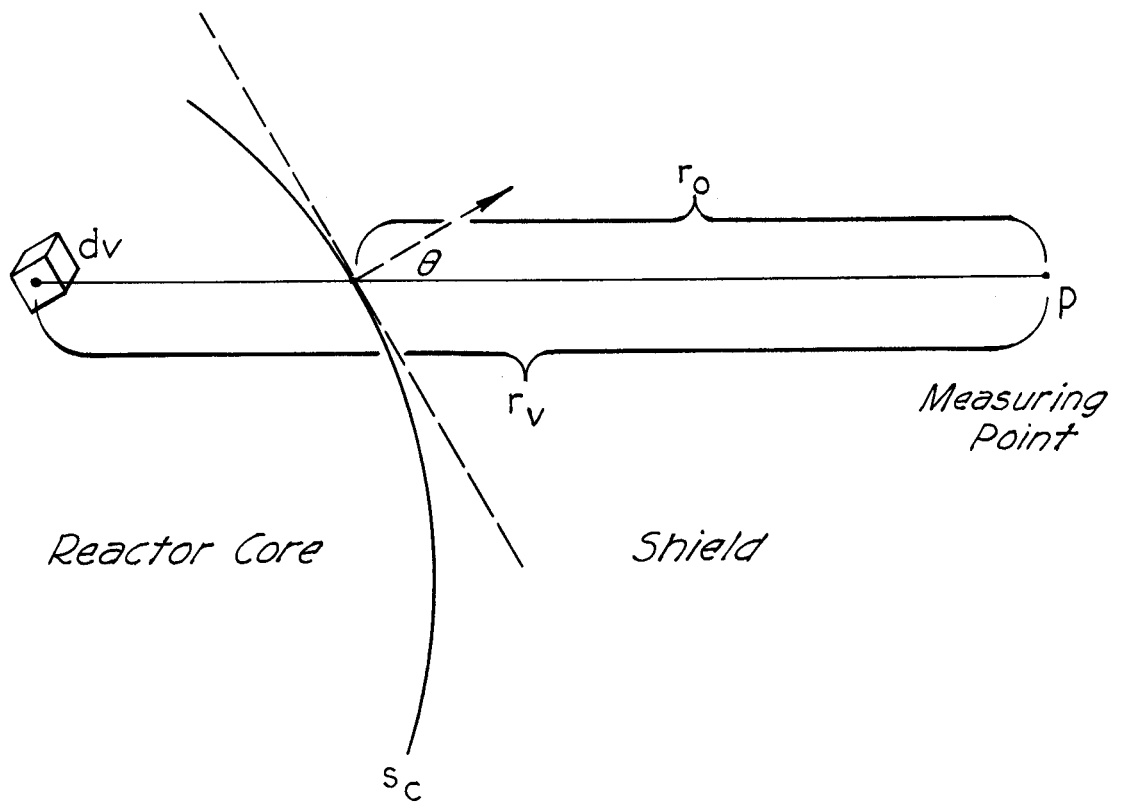


Fig. 7

~~CONFIDENTIAL~~

The upper limit for r_v is taken as infinity for simplicity. If the core diameter is larger than $2\lambda_c$, then this will introduce an error no greater than about 10%. This condition is usually well fulfilled. If it is not, then a method derived in connection with the "fast effect" is applicable.⁷⁻⁹

In reactors which are used for power production it is usually desirable to keep the heat release density, p , constant over the volume. For this case the second integral is easily evaluated. For

$$p(r_v) = p_0 = \text{constant},$$

$$D = \text{const.} \approx \lambda_c p_0 \int_{s_c} G(r_0) ds_c . \quad (25)$$

In other words, for constant power density in the core the equivalent surface source strength is simply $\lambda_c p_0$ watts/cm², and

$$\sigma_{\text{equiv.}} = \lambda_c p_0 . \quad (26)$$

It might be noted at this point that Eq. (26) is at variance with the familiar result for leakage from the surface of a radioactive self-absorbing semi-infinite volume source, to wit $N_0\lambda/4$ (particles per unit source area per unit time) where N_0 is the activity per unit volume. The difference lies in two places. In the present discussion a milligoat detector is used, which would read $N_0\lambda/2$, which is not the leakage at all. The second difference arose from the neglect of the cosine factor in Eq. (23). This means that Eq. (26) describes a source which is isotropic but matched to the actual cosine source in the normal direction. This makes only negligible error for thick shields.

~~SECRET~~

For the case in which the power can be represented as a constant plus a cosine function the equivalence is again easily derived if the core diameter is large compared to λ_c :

$$p(r_v) = P_0 + p_1 \cos \left[\frac{\pi}{2} \left(1 - \frac{r_v - r_0}{a} \right) \right] \quad (27)$$

$$= P_0 + p_1 \sin \left(\frac{\pi}{2} \frac{r_v - r_0}{a} \right), \quad (27a)$$

where a is the core half-width.

Equation (27) can be approximated near the core surface, using the argument to replace the sine, by the following expression:

$$p(r_v) \approx P_0 + p_1 \frac{\pi}{2a} (r_v - r_0). \quad (28)$$

For this case, Eq. (24) becomes

$$D = \left(\lambda_c P_0 + p_1 \frac{\pi \lambda_c^2}{2a} \right) \int_{s_c} G(r_0) ds_c, \quad (29)$$

whence

$$\sigma_{equiv.} = \left(\lambda_c P_0 + \lambda_c^2 \frac{\pi}{2a} p_1 \right). \quad (30)$$

The source strengths represented by Eqs. (26) and (30) are appropriate for use with the transformations in the previous section.

~~SECRET~~

Comparison of Lid Tank and BSF Water Data

It is possible to determine the point-to-point attenuation kernel for water from either Lid Tank or BSF data, using the methods which have just been described. Alternately, it is possible to predict from the Lid Tank data what is to be expected in the BSF. As an example of the method the latter will be carried out.

The first step is to transform the Lid Tank data for fast neutrons to the point-to-point kernel. This can be done using Eq. (6) for the smaller values of z , but it will be seen that knowledge of $G(z)$ requires observed values of dose for distances greater than z . Thus, while the method of Eq. (6) can be used for z up to about 80 cm, another method is required beyond this distance.

The attenuation in water is great enough so that the expression need be accurate only for the nearest point of the source, an approximation being quite adequate for the rest.

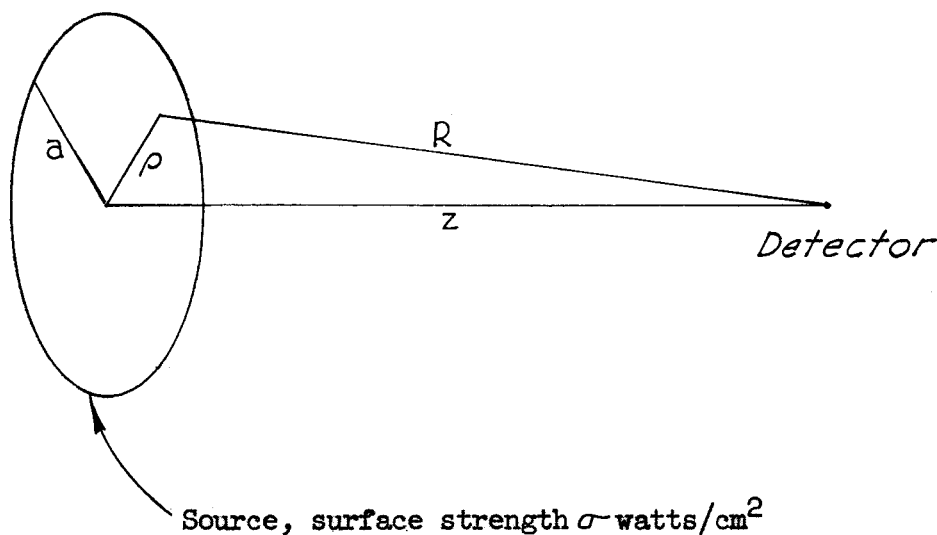


Fig. 8. Lid Tank Geometry

For the Lid Tank source, a circular disc, the dose is given by

$$D(z,a) = 2\pi\sigma \int_{\rho=0}^a G(R) \rho d\rho. \quad (31)$$

Applying the approximation given in Eq. (13) for $G(R)$, and expanding R , that is,

$$G(R) \cong G(z) e^{-(R-z)/\lambda},$$

$$R \sim z + \frac{\rho^2}{2z},$$

$\lambda = \lambda(z)$, determined directly from the slope of $D(z,a)$.

$$\begin{aligned} D(z,a) &= 2\pi\sigma G(z) \int_{\rho=0}^a e^{-\frac{\rho^2}{2\lambda z}} \rho d\rho \\ &= 2\pi\sigma \lambda z G(z) \left(1 - e^{-\frac{a^2}{2\lambda z}}\right) \end{aligned} \quad (32)$$

Equation (32) gives the relation between point-to-point kernel, $G(z)$, and observed dose, $D(z,a)$, for the Lid Tank, and agrees within less than two percent with the more careful determinations by Eq. (6).

To enable comparison with calculations, $4\pi z^2 G(z)$ is plotted in Fig. 9, which represents the dose which would be observed with an infinite collimated source

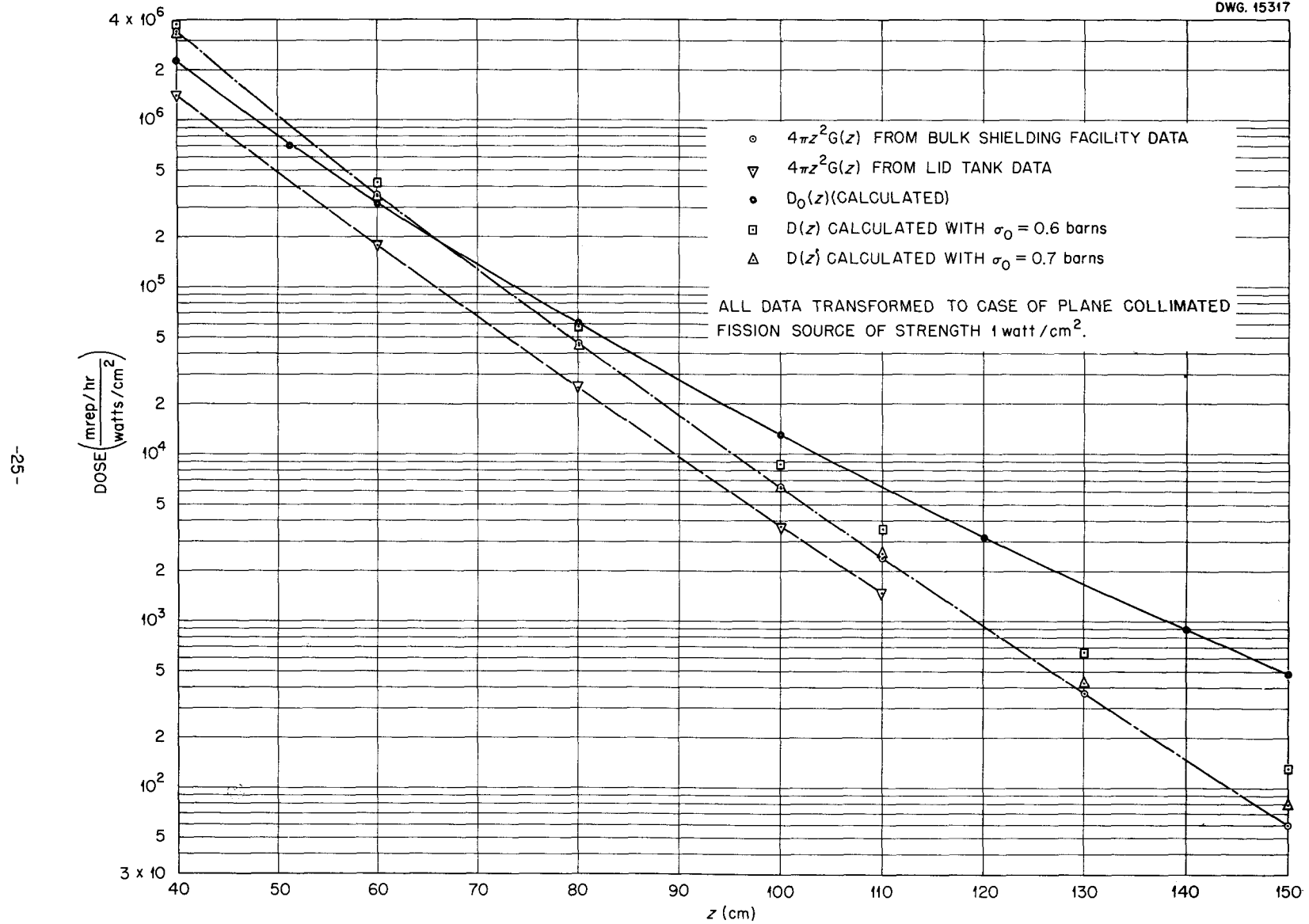


Fig. 9. Comparison of Neutron Dose Calculations with Experiment for a Water Shield.

~~SECRET~~

of unit strength.* The source strength used in Eq. (32) was obtained by dividing the power (6 watts) by the source area (3970 cm²) and dividing this quotient by the attenuation to be ascribed to the several layers of material which are permanently over the source. This latter division has been calculated many times to be 1/0.6, i.e., of the neutrons which would have entered the water more or less normally, only 0.6 of these actually do reach the water owing to collisions in the source support and tank walls (Fig. 3). Thus the original data¹⁰ was multiplied by 1.1×10^{-3} .

The BSF data does not lend itself so easily to reduction to a simple form. The shape of the reactor, its composition, and its power distribution must all be considered. The general method, however, is the same as that used for the Lid Tank.

The power distribution has been measured by means of gold foils,¹¹ and a simple fit to the power distribution on the north face of the pile was found. In the -z direction, that is, into this face, the power level was taken as constant.

* Actually the transformation from point source reading to plane collimated source, here assumed to consist merely of multiplying by $4\pi z^2$, is not rigorous, but is assumed adequate in a highly attenuating medium such as water, in which very little contributing radiation has suffered large angle scattering.

~~SECRET~~

The measurements seem to indicate this to be the case for the first 8 cm. In the x and y directions simple parabolae were fitted to the power distribution. Power density in the core was corrected by a factor of 200/165 to take account of the fact that Meem and Johnson used 165 Mev/fission, whereas 200 is probably better for the reactor, which self-absorbs most of the gammas and betas. The surface strength was taken to be product of power density and a relaxation length for the core. The latter was obtained from estimates of the removal cross section for the metal of the reactor, and the water of the core was credited with an attenuation length which was observed, as a function of z, in the Lid Tank.

Thus

$$\frac{1}{\lambda_{\text{core}}(z)} = 0.036 + \frac{0.58}{\lambda(z)} . \quad (33)$$

The dose in the water around the BSF reactor, at a distance z from the center of the north face, is

$$D(z) = \lambda_c \int_{-a}^a dx \int_{-b}^b dy p(x,y) G(R) , \quad (34)$$

$$p(x,y) = P_0(1 - \lambda x^2)(1 - \beta y^2) ,$$

P_0 , the power at the center of the north face, is equal to 1.88×10^{-5} watts/cm³,

$$\lambda = 1.5 \times 10^{-3} \text{ cm}^{-2} ,$$

$$\beta = 7 \times 10^{-4} \text{ cm}^{-2} ,$$

a, b are the half lengths of the north face.

After making the usual approximations, it is found that

$$D(z) = \lambda_c G(z) P_0 \int_{-a}^a dx \int_{-b}^b dy e^{-\frac{x^2}{2\lambda z} - \frac{y^2}{2\lambda z}} (1 - \alpha x^2) (1 - \beta y^2),$$

$$D(z) = 2\pi G(z) P_0 \lambda_c \lambda z f(2\lambda z), \quad (35)$$

$$\text{where } f(2\lambda z) = \left[\text{Erf} \left(\frac{a}{\sqrt{2\lambda z}} \right) - 2\alpha \lambda z \left(\frac{1}{2} \text{Erf} \left(\frac{a}{\sqrt{2\lambda z}} \right) - \frac{a}{\sqrt{2\pi\lambda z}} e^{-\frac{a^2}{2\lambda z}} \right) \right] \times$$

$$\times \left[\text{Erf} \left(\frac{b}{\sqrt{2\lambda z}} \right) - 2\beta \lambda z \left(\frac{1}{2} \text{Erf} \left(\frac{b}{\sqrt{2\lambda z}} \right) - \frac{b}{\sqrt{2\pi\lambda z}} e^{-\frac{b^2}{2\lambda z}} \right) \right].$$

This expression has been evaluated using the $G(z)$ obtained from the analysis of the Lid Tank data. Comparison with the actual BSF data¹² shows the latter to be higher by a factor varying from about 1.6 at 110 cm to 2.4 at 40 cm. It is not surprising that the discrepancy is greater at 40 cm, since the approximations are less accurate at smaller z . The average discrepancy, however, must be attributed in large measure to inaccuracies of intercalibration of source strengths. The detectors are probably in good agreement. The effective Lid Tank source is not easy to define since its strength varies over its surface because of two structure effects, one attributable to the cylinders which make up the source, the other to the long holes in the graphite reactor lattice which cause rather strong beams of neutrons to emerge. These are not entirely smoothed out by the time the source

[REDACTED]

plate is reached.

Residual discrepancies of the size here encountered are commonly found in shielding calculations. It seems to be the case that the amount of experimental and theoretical work necessary to resolve such discrepancies, even in a simple geometry, is entirely disproportionate to any possible resulting practical gain.

~~SECRET~~

METHOD OF DIRECT CALCULATION

Although the method of direct comparison is very convenient and reliable when the appropriate experiment is available, a second method of shield computation is useful for quick estimates when no comparison experiment has been done. The method to be described can in some ways be regarded as a theoretical prediction of shield attenuation. It will be clear, however, that the present lack of detailed cross-section information enforces such strong dependence of theory on attenuation measurements that this second method of calculation is to be regarded as another comparison method, albeit somewhat more flexible than the first.

The pictorial basis for this second method has already been given in (I), and need here be only briefly reviewed. The concept of removal cross-section was introduced in (I) as being the cross-section for a collision which renders a neutron incapable of contributing to the neutron dosage outside the shield. All shields to be discussed have the property that the hydrogen content is sufficient to render an inelastic collision equivalent to absorption. A neutron collision with hydrogen is nearly always equivalent to absorption, and the small fraction of ineffective hydrogen collisions will be taken into account by a slowly varying build-up factor. Isotropic elastic scattering on elements other than hydrogen is nearly equivalent to absorption, unless it occurs in an improbable location. Finally, anisotropic elastic "shadow" scattering is only partially equivalent to absorption, the fraction depending on neutron energy, shield composition, and collision location in a complicated way, so that recourse to experiment is here essential.

The simplest neutron shield is a mass of pure hydrogen, in which the attenuation could be calculated from first principles. Lacking this simplest case, it is very convenient to use water as the prototype neutron shield. As is clear

[REDACTED]

from an earlier section, the measurements in water are easy to perform, so that a large body of reliable data exists. The oxygen, which is the chief difficulty in calculation, does not play a dominant role, so that a simplified treatment is possible.

The following procedure will be used. First the uncollided neutron flux will be calculated, for a simple geometry and assuming zero cross-section for oxygen. This calculation is an extension of the one which led to Eq. (17) of (I). A removal cross-section will then be introduced for the oxygen in order to make the uncollided flux equal the observed fast flux. Small corrections will then be made to this removal cross-section by introducing a build-up factor for fast flux (neutron dose) and another factor for thermal flux.

Calculation of Uncollided Flux

By means of the geometrical transformation described in an earlier section, the lid tank neutron measurements for water have been transformed to the collimated plane source form, and this form will here be used. Imagine an infinite plane fission source located in the x-y plane of a system of rectangular coordinates. The source strength will be taken as one neutron per square centimeter per second. The fissions are assumed to emit neutrons normally in the direction of the positive z-axis. The macroscopic hydrogen cross-section for water is (Eq. (14), I):

$$\sum_H = \frac{0.735}{E + 1.66} \text{ cm}^{-1} = \frac{\beta}{E + \epsilon} \quad (E \text{ in MEV}) \quad (36)$$

Several convenient expressions for the fission spectrum were given in (I), but for present purposes still another form seems best to combine convenience and accuracy. From Eq. (2) of (I), the fraction of neutrons per MEV emitted from a U^{235} fission is:

$$N(E) = \frac{1}{\sqrt{2\pi e}} e^{-(E-\sqrt{2E})} = 0.242 e^{-(E-\sqrt{2E})} \quad (37)$$

A very good fit to the exponent of Eq. (37) is:

$$E - \sqrt{2E} \cong \alpha E + \frac{\beta \mathcal{J}}{E + \epsilon} - \gamma \quad (38)$$

$$\alpha = 0.813 \text{ MEV}^{-1}$$

$$\mathcal{J} = 7.35 \text{ cm}$$

$$\gamma = 3.05$$

Using Eqs. (36) and (38), and proceeding as was done for Eq. (15) of (I), the uncollided flux of neutrons at distance z from the source (neglecting all cross-sections save that of hydrogen) will be:

$$S(E, z) = 5.12 e^{-\alpha E} e^{-\frac{\beta(z+\mathcal{J})}{E+\epsilon}} \quad (39)$$

Analogously to (I), the energy of the maximum of this spectrum will be:

$$E_0 = \left[\frac{\beta(z+\mathcal{J})}{\alpha} \right]^{\frac{1}{2}} - \epsilon \quad (40)$$

In order to find the total uncollided flux, an integral must be done over all energies. The simplest procedure is the so-called saddle-point method, which approximates the integrand by a Gaussian function around its maximum. For this purpose, write:

$$f(E) = \alpha E + \frac{\beta(z+\mathcal{J})}{E+\epsilon} = f(E_0) + f'(E_0)(E-E_0) + \frac{1}{2} f''(E_0)(E-E_0)^2$$

where:

$$f(E_0) = 2 \sqrt{\alpha \beta (z + \delta)} - \alpha E$$

$$f'(E_0) = 0$$

$$f''(E_0) = 2 \sqrt{\frac{\alpha^3}{\beta (z + \delta)}}$$
(41)

The integrated uncollided flux is now:

$$\phi_0(z) = 5.12 \alpha E e^{-2 \sqrt{\alpha \beta (z + \delta)}} \int_0^\infty dE e^{-\frac{1}{2} f''(E_0) (E - E_0)^2}$$
(42)

The integral can obviously be extended to $-\infty$ for not too small values of E_0 , and $\phi_0(z)$ then becomes:*

$$\phi_0(z) = 17.3 \sqrt{\pi} e^{-2 \sqrt{\alpha \beta (z + \delta)}} \left[\frac{\beta (z + \delta)}{\alpha^3} \right]^{\frac{1}{4}}$$

$$= 33.2 (z + \delta)^{\frac{1}{4}} e^{-1.547 \sqrt{z + \delta}}$$
(43)

This result is basic for the further developments of this section.

For ease in obtaining results for actual shields, it will be convenient to make use of the fact that fast neutron flux is very nearly proportional to dose. The standard source unit will further be taken as one watt/cm² of fission energy.

* In connection with the question of the accuracy to be expected from the procedure here used, the following may be of interest. If the fission spectrum is taken to be $E^{-\frac{1}{2}} e^{-\alpha E}$ and \sum is taken as β/E , the integral of (41a) can be done exactly, yielding $\sqrt{\frac{\pi}{\alpha}} e^{-2 \sqrt{\alpha \beta z}}$. Consistent application of the above approximation method (with the additional prescription that the slowly varying factor $E^{-\frac{1}{2}}$ is to be evaluated at $E = E_0$ and taken outside the integral) yields exactly the same answer.

Using:

$$1 \text{ watt} = 3 \times 10^{10} \text{ fission/sec.}$$

$$\nu = 2.5 = \text{number of neutrons emitted per } U^{235} \text{ fission}$$

$$1 \frac{\text{neutron}}{\text{cm}^2\text{-sec.}} = 1.44 \times 10^{-2} \frac{\text{mrep}}{\text{hour}}$$

and defining $D_0(z)$ as the uncollided dose in $\frac{\text{mrep}}{\text{hour}}$ from a collimated U^{235} fission source of strength one watt/cm², Eq. (43) then becomes:

$$D_0(z) = 3.6 \times 10^{10} (z + d)^{\frac{1}{4}} e^{-1.547 \sqrt{z+d}} \frac{\text{mrep.}}{\text{hour}} / \frac{\text{watt}}{\text{cm}^2} \quad (44)$$

This function is plotted in Fig. (9), where it is compared with the function $4\pi z^2 G(z)$ previously derived from the lid tank dosimeter data. The calculated function is too high by a factor of about 1.6 at 40 cm. This excess steadily becomes worse, until a ratio of 4.2 is reached at 110 cm. This increasing discrepancy arises from two partially compensating neglects in the derivation of Eq. (44). The first neglect is the omission of dosage rate produced by neutrons which have made a hydrogen collision but have not been stopped at the point of observation. The second neglect is the inclusion of dosage rate produced by neutrons which have been deflected by an oxygen collision and therefore lost, because of the increased distance of travel to the point of observation.

Correction for Hydrogen Build-up and Oxygen Removal

In the phenomenological theory to be developed, the first difficulty will be handled by the use of a simple build-up factor, while the second will be treated by an experimental adjustment of the oxygen removal cross-section. A really complete calculation of these effects must include their interaction, which leads to mathematical work of rather complex type. A great simplification (of admittedly

~~SECRET~~

unknown validity) will here be made by separating the two effects. Since the basic curve D_0 already agrees fairly well with experiment, it is very reasonable to expect that the two neglected effects are separately small, and that their interaction can therefore be ignored. This notion can be incorporated in the following pair of assumptions.

1. The oxygen attenuation effect will be described by an energy-independent (for a first trial) removal cross-section, and the hydrogen build-up will accordingly be calculated for a system containing only a constant absorption cross-section, in addition to the hydrogen scattering cross-section.

2. In discussion of the oxygen attenuation, the hydrogen scattering will similarly be considered as simple absorption.

The existence of the hydrogen build-up implies that the integrand of Eq. (42) is to be multiplied by a slowly varying function of z and E , which takes into account the residual effectiveness of neutrons which have made a hydrogen collision. It is actually convenient (and essentially rigorous) to evaluate this function at $E_0(z)$, the energy of the peak of the uncollided spectrum. This brings a simple function of z in as a multiplying factor. This function will be called $B(z)$.

To take the oxygen attenuation into account, the uncollided dose is to be multiplied by a factor $e^{-\sum_0 z}$, where \sum_0 is a macroscopic oxygen removal cross-section. The true dose function which will replace D_0 is then:

$$D(z) = e^{-\sum_0 z} B(z) D_0(z) \quad (45)$$

The product form is the essential expression of the assumption of no interaction between the hydrogen build-up and oxygen attenuation.

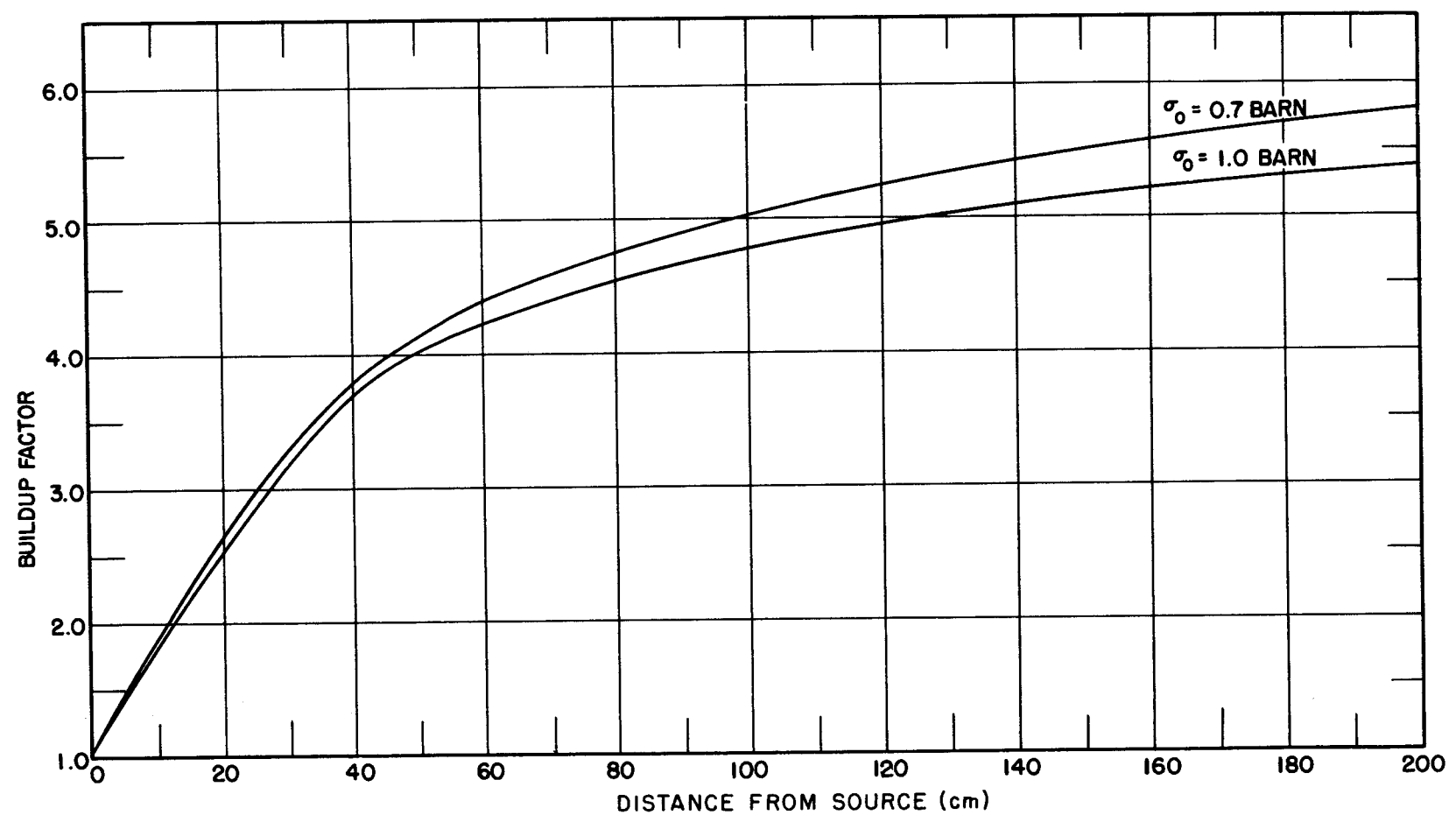
~~SECRET~~

Since $B(z)$ depends (not very sensitively) on Σ_0 , a rough guess must be made for this quantity in order to calculate $B(z)$. The Eq. (45) can then be compared with experiment to obtain a value for Σ_0 . A rough calculation of $B(z)$ is described in an appendix and the curves are given in Fig. 10 for two values of Σ_0 , corresponding to microscopic cross-sections of 0.7 and 1.0 barn.

These curves exhibit some interesting features. The build-up starts at unity for z equal to zero, as it must. It then rises rapidly to a value of about four, with a slow further rise. This further rise continues indefinitely, but at a continually falling rate. The initial rise can be thought of as due to the coming of the degraded spectrum into approximate equilibrium with the uncollided spectrum. If this equilibrium were really achieved, a monoenergetic uncollided flux would be multiplied by a constant to give the total flux. As is well known, such a true equilibrium can never be reached, because of the presence of collided neutrons which have been deflected by arbitrarily small angles and are essentially indistinguishable from uncollided neutrons. This phenomenon is responsible for the slow asymptotic rise of the build-up for a monoenergetic source.

In Fig. 9 is also plotted the function $D(z)$ with $\sigma_0 = 0.6$ and 0.7 barns. For the calculation of the insensitive $B(z)$, 0.7 barns was assumed. It is seen that both curves are higher than the corresponding curve derived from the lid tank data. For $\sigma_0 = 0.7$ barns, however, agreement is essentially perfect with the BSF data, up to $z = 110$ cm. A very slight increase of σ_0 (~ 0.01 barn), combined with a small increase of the source strength would give excellent agreement over the whole range plotted. It is felt, however, that such fine adjustments really are not in the spirit of so rough a theory, and the approximate figure of 0.7 barns will be taken as the effective removal cross-section for oxygen.

DWG. 12767



-37-

Fig. 10. Neutron Buildup in Water as a Function of Distance from Source for Two Values of Oxygen Cross Section.

~~SECRET~~

It is interesting to compare this result with a similar one obtained by Blizard and Enlund¹³ using the thermal neutron data from the Lid Tank. This calculation differs from the dose calculation principally in the method used for handling the hydrogen build-up. The method already described will be completely unreliable for the build-up of thermal flux (it is not highly reliable for the build-up of neutrons above 1 MEV!). The thermal build-up is therefore calculated using a modification of age theory for handling the slowing down problem.

The uncollided flux as a function of energy was represented essentially as in the methods previously described. A constant oxygen removal cross-section was included in this preliminary calculation. The oxygen-collided neutrons were assumed to emerge isotropically, without energy loss. This source was then convoluted with a Gaussian approximation to the water slowing down kernel, using a calculated age.¹⁴

Each hydrogen-collided neutron was assigned an age corresponding to its collision-degraded energy, using the same data. The energy-angle correlation for the hydrogen-collided neutrons was qualitatively taken into account by convoluting the angle-integrated source of such neutrons with a Gaussian displacement kernel which displaced only outwardly (in the positive z-direction), not radially from the point of collision. The form of the kernel used was:

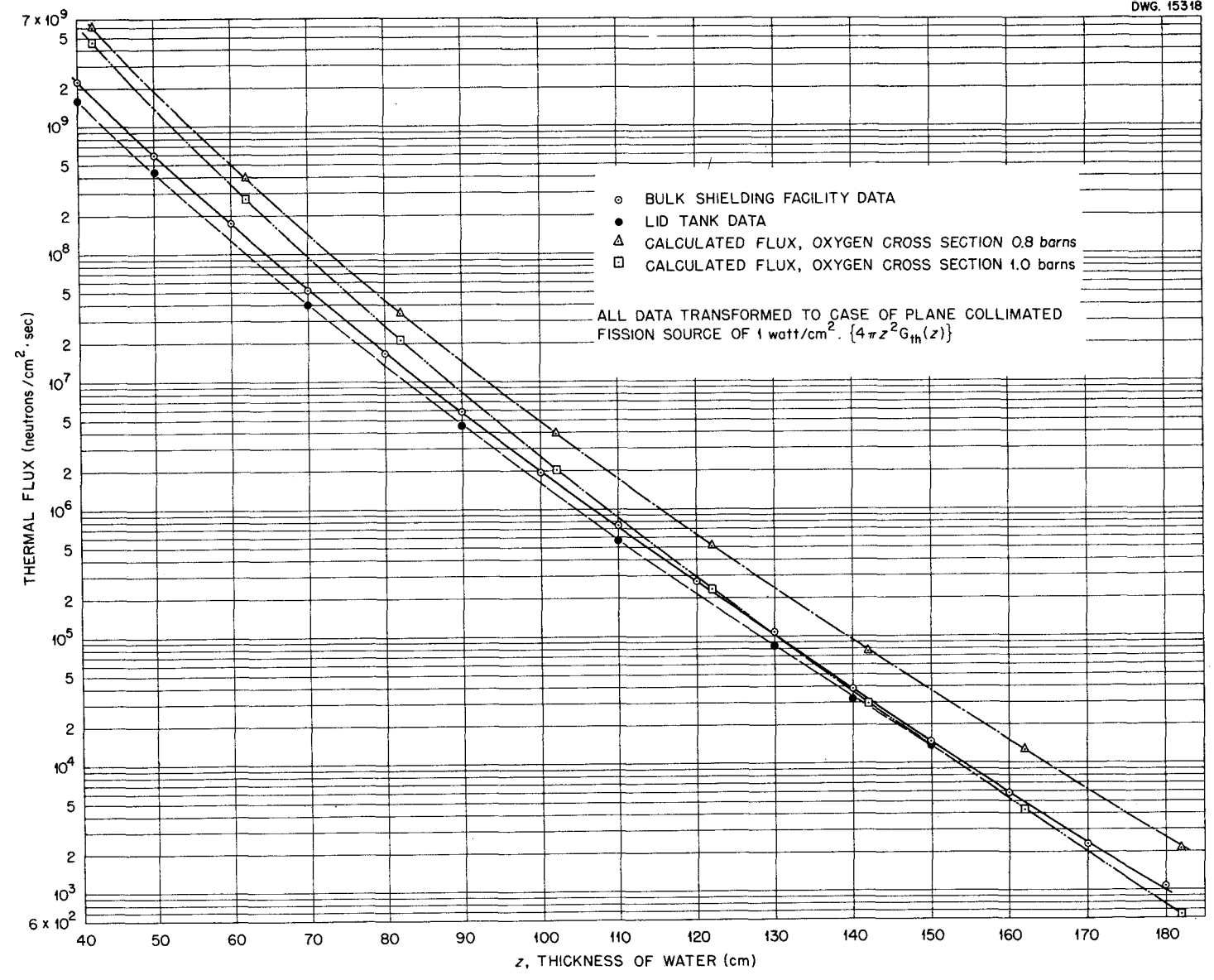
$$\begin{aligned}
 (z' - z)^2 e^{-(z' - z)^2 / 4\tau} & \quad z' > z \\
 0 & \quad z' < z
 \end{aligned}
 \tag{46}$$

The displacement due to thermal diffusion was simply added to all values of z.

~~SECRET~~

Fig. 11 shows the thermal flux data for a plane collimated source, $4\pi z^2 G_{Th}(z)$. The curves are shown for the transformed Lid Tank¹⁵ and Bulk Shielding Facility¹² data, as well as the calculated curves for $\sigma_0 = 0.8$ and 1.0 barn. It is to be noted that $\sigma_0 = 0.8$ yields a better fit to the shape. The previously noticed discrepancy between the two sets of experimental data shows up here also, although the ratio is closer to one for the thermal data.

The two best values of σ_0 obtained from the dose data and the thermal data presumably differ because of the non-comparable treatments of hydrogen build-up and probably also because of the somewhat slippery character of the removal cross-section concept. For all practical purposes, either one (or a compromise value) will give excellent results for useful shield thicknesses.



- 40 -

Fig.11. Comparison of Thermal Flux Calculations with Experiment for a Water Shield.

~~SECRET~~

References

1. E. P. Blizard and T. A. Welton, "The Shielding of Mobile Reactors I," Reactor Science and Technology 1, No. 3, 15 (Dec. 1951); ORNL-1133.
2. T. A. Welton, A Review of Analytical Methods for the Calculation of Neutron and Gamma-Ray Attenuations, TID-256 (Oct. 5, 1949).
3. G. H. Peebles, Gamma-Ray Transmission Through Finite Slabs - Part I, RM-653 (July 23, 1951).
4. L. V. Spencer and U. Fano, Phys. Rev. 81, 464 (1951); J. Research Nat'l. Bur. Stand. 46, 446 (1951).
5. H. Goldstein and J. E. Wilkins, L. V. Spencer and U. Fano, Phys. Rev. (in press).
6. C. E. Clifford, The ORNL Shield Testing Facility, ORNL-402 (Nov. 4, 1949); or see his article in Theoretical and Practical Aspects of Shielding, ORNL-710, p. 193 (Sept. 29, 1950).
7. H. Castle, H. Ibser, G. Sacher, and A. M. Weinberg, The Effect of Fast Fission on k, CP-644 (May 4, 1943).
8. F. H. Murray, Fast Effects, Self-Absorption, Fluctuation of Ion Chamber Readings, and Statistical Distribution of Chord Lengths in Finite Bodies, CP-2922 (Apr. 6, 1945).
9. S. Kushnerink, Absorption of Gamma Rays by Homogeneous Cylinders Containing Uniform Source Distributions, TPI-46 (May 6, 1947).
10. C. E. Clifford, E. P. Blizard et al., in ANP Quarterly Report ORNL-919, p. 132 (Feb. 26, 1951).
11. J. L. Meem and E. B. Johnson, Determination of the Power of the Shield-Testing Reactor, ORNL-1027, (Aug. 13, 1951).
12. R. G. Cochran and H. E. Hungerford, Fast Neutron Dosimeter Measurements for Experiment 1 in the Bulk Shielding Facility, ORNL CF-51-5-61 (May 7, 1951); H. E. Hungerford, Bulk Shielding Facility Water Data Work Sheet, ORNL CF-52-2-37; J. L. Meem et al., ANP Quarterly Report ANP-65, p. 113; E. P. Blizard, Introduction to Shield Design II, ORNL CF-51-10-70, part 2, p. 92.
13. E. P. Blizard and H. L. F. Endlund, Physics Division Quarterly Report, ORNL-1216, p. 20.
14. N. M. Dismuke and M. R. Arnette, Mon P-219.

- ~~CONFIDENTIAL~~
15. E. P. Blizard, C. E. Clifford, et al, Physics Division Quarterly Report, ORNL-1107, p. 3.
 16. G. C. Wick, Phys. Rev. 75, 738 (1949).
 17. S. Podgor, ORNL-1130.

APPENDIX - NEUTRON BUILD-UP IN HYDROGEN

A simple, approximate treatment of the neutron build-up in hydrogen is possible, along lines suggested by G. C. Wick^{2,16}. The fundamental Boltzmann equation for the problem is:

$$\begin{aligned} \cos \vartheta \frac{\partial \psi}{\partial z} + (\Sigma_H + \Sigma_R) \psi \\ = \frac{1}{2\pi} \int_E^\infty \frac{dE'}{E'} \Sigma_H(E') \int d\vartheta' \psi(z, E', \vartheta') \int (\sqrt{\frac{E}{E'}} - \cos |\vartheta - \vartheta'|) \\ + \int (E - E_0) \int(z) \int(\vartheta) \end{aligned} \quad (1)$$

ψ = flux of neutrons at distance z from the source, per unit range of energy, and per unit solid angle.

ϑ = angle between neutron velocity and the z direction.

Σ_H = the macroscopic hydrogen cross-section.

Σ_R = any other "removal" cross-section, to be taken as equivalent to absorption, and as independent of energy.

ϑ = vector specifying direction (including azimuth) of neutron velocity.

$d\vartheta'$ = element of solid angle.

$|\vartheta - \vartheta'|$ = deflection angle in a neutron collision.

$\int(\vartheta)$ = function having value only for ϑ ($= |\vartheta|$) = 0 and unit integral over angle.

The last term in Eq. (1) describes a source which is plane ($z = 0$), mono-energetic and mono-directional ($\vartheta = 0$).

~~SECRET~~

Although this rather general equation can be solved with any energy dependence of \sum_H and \sum_R , by methods now available^{3,4,5}, a modification of the approximate method given by Wick for large z will be used here. The method originally given by Wick for determining the asymptotic behavior of the neutron density actually goes through more naturally for the case of γ -ray penetration. The neutron treatment given here is accordingly modified so that it is much more closely parallel to the γ -ray calculation than is Wick's work. The advantage gained is two-fold. First, the energy dependence of the hydrogen cross-section turns out to be more realistic than Wick's. Second, the interaction of cross-section change with energy and the change in penetration with increasing angle is here included. Several compromises must be made on other points, but it is believed that the overall treatment is good to lower energies than existing treatments of this general type. Define a variable u :

$$u(E) = \int_E^{E_0} \frac{dE'}{E'} \frac{\sum_H(E')}{\sum_H(E_0)} \quad (2)$$

and approximate $\sum_H + \sum_R$ by the first two terms in a series expansion in powers of u :

$$\sum_H + \sum_R = \Sigma = \Sigma(0) [1 + \alpha u] \quad (3)$$

Choose a new length unit $x = \Sigma(E_0)z$ and write:

$$\beta = \frac{\sum_H(E_0)}{\Sigma(E_0)} \quad (4)$$

The flux will be calculated only for fairly small angles of travel so that:

$$\cos \varrho = 1 - \frac{\varrho^2}{2}$$

$$\cos \left| \underline{\varrho} - \underline{\varrho}' \right| = 1 - \frac{1}{2} \left| \underline{\varrho} - \underline{\varrho}' \right|^2 \quad (5)$$

Finally, the quantity $\sqrt{\frac{E}{E'}}$ will be expanded in a double power series in u and u' , and only the first order terms retained:

$$\sqrt{\frac{E}{E'}} = 1 - \frac{1}{2}(u - u') \quad (6)$$

The fundamental Eq. (1) then becomes:

$$\begin{aligned} \left(1 - \frac{\varrho^2}{2}\right) \frac{\partial \psi}{\partial x} + (1 + \alpha u) \psi &= \frac{\beta}{2\pi} \int_0^u du' \int d\underline{\varrho}' \psi(x, u', \underline{\varrho}') \int \left(\frac{|\underline{\varrho} - \underline{\varrho}'|^2}{2} - \frac{u - u'}{2}\right) \\ &+ \frac{1}{E_0} \int(u) \int(x) \int(\underline{\varrho}) \end{aligned} \quad (7)$$

With the approximations made to obtain Eq. (7), $\underline{\varrho}$ can be thought of as a two-dimensional vector with magnitude ϱ . It is convenient to make a Fourier transform on x , a Laplace transform on u , and a two-dimensional Fourier transform on $\underline{\varrho}$:

$$\phi(k, \eta, S) = \frac{1}{8\pi^3} \int_{-\infty}^{\infty} dk e^{-ikx} \int d\underline{s} e^{-i\underline{s} \cdot \underline{\varrho}} \int_0^{\infty} du e^{-\eta u} \psi(x, u, \underline{\varrho}) \quad (8)$$

The transform of Eq. (7) then is:

$$\left(1 - K - \alpha \frac{\partial}{\partial \eta}\right) \phi - \frac{1}{2} \frac{\partial^2 \phi}{\partial S^2} = \frac{\beta}{\eta} e^{-\frac{S^2}{4\eta}} \phi + \frac{1}{E_0} \quad (9)$$

$$K = -ik$$

Transform from the variables (η, s) to (η, t) , where:

$$\frac{s^2}{2\eta} = t^2 \quad (10)$$

and write:

$$\chi = e^{-\frac{\alpha t^2}{2}} \phi \quad (11)$$

Eq. (9) then becomes:

$$\left(\frac{\partial^2}{\partial t^2} + \frac{1}{t} \frac{\partial}{\partial t} + 2\alpha - \alpha^2 t^2 + 4\beta e^{-\frac{t^2}{2}} \right) \chi - 4\eta (1 - \kappa - \alpha \frac{\partial}{\partial \eta}) \chi = -\frac{4\eta}{E_0} e^{-\frac{\alpha t^2}{2}} \quad (12)$$

Wick's procedure at this point is to expand χ in a series of orthogonal functions of t :

$$\chi(\eta, t, \kappa) = \sum_n \chi_n(\eta, \kappa) U_n(t) \quad (13)$$

where:

$$\left(\frac{d^2}{dt^2} + \frac{1}{t} \frac{d}{dt} + 2\alpha - \alpha^2 t^2 + 4\beta e^{-t^2/2} \right) U_n = \lambda_n U_n \quad (14)$$

so that:

$$\begin{aligned} 4\alpha \eta \frac{d\chi_n}{d\eta} + \left[\lambda_n - 4\eta (1 - \kappa) \right] \chi_n &= -\frac{4\eta}{E_0} \frac{\int_0^\infty U_n e^{-\frac{\alpha t^2}{2}} t dt}{\int_0^\infty U_n^2 t dt} \\ &= -\frac{4\eta}{E_0} Q_n \end{aligned} \quad (15)$$

This equation has the solution:

$$\chi_n = \frac{Q_n}{\alpha E_0} e^{-\frac{1-K}{\alpha} \eta} \eta^{-\frac{\lambda_n}{4\alpha}} \int_0^{\infty} d\eta' e^{-\frac{1-K}{\alpha} \eta'} \eta'^{\frac{\lambda_n}{4\alpha}} \quad (16)$$

For large z and u , it can be shown that only the behavior of χ_n for small η is important. It is also then true that only the term $n = 0$, corresponding to the highest possible value of λ_n , contributes. Under these conditions, and omitting the subscript:

$$\chi = \frac{Q}{\alpha E_0} \Gamma(n+1) \left(\frac{\alpha}{1-K} \right)^{n+1} e^{\frac{1-K}{\alpha} \eta} \eta^{-n} \quad (17)$$

$$n = \frac{\lambda}{4\alpha}$$

A good value for λ , as well as a reasonable approximation for U , can be obtained by assuming U to have a Gaussian shape and then utilizing the Ritz method.

Write:

$$U = e^{-\frac{\gamma t^2}{2}} \quad (18)$$

and

$$\lambda = \frac{\int_0^{\infty} t dt \left[(2\alpha - \alpha^2 t^2 + 4\beta e^{-\frac{t^2}{2}}) U^2 - \left(\frac{dU}{dt} \right)^2 \right]}{\int_0^{\infty} t dt U^2} \quad (19)$$

where γ is so chosen as to maximize λ .

This procedure yields:

$$\lambda = 2\alpha - \frac{\alpha^2}{\gamma} - \gamma + \frac{8\beta\gamma}{2\gamma+1} \quad (20)$$

where γ is given by

$$\frac{\alpha^2}{\gamma^2} + \frac{8\beta}{(2\gamma+1)^2} - 1 = 0 \quad (21)$$

The multiple transform ϕ is then given by:

$$\phi(k, \eta, s) = \frac{2\gamma\Gamma(n+1)}{\alpha(\alpha+\gamma)E_0} \left(\frac{\alpha}{1-K}\right)^{n+1} e^{\frac{1-K}{\alpha}\eta} \eta^{-n} e^{\frac{\alpha-\gamma}{4\eta}s^2} \quad (22)$$

For purposes of calculating dosage, the integral over angle of ψ will be found and called $\bar{\psi}$. It is given by:

$$\bar{\psi}(x, u) = \frac{2\gamma}{\alpha+\gamma} \Gamma(n+1) \frac{\alpha^n}{E_0} \frac{1}{2\pi} \int_{-\infty}^{\infty} dk \frac{e^{ikx}}{(1+ik)^{n+1}} \frac{1}{2\pi i} \int_{-i\infty}^{i\infty} d\eta e^{\eta u} \eta^{-n} \quad (23)$$

The integrals in Eq. (23) are easily done, yielding:

$$\bar{\psi}(x, u) = \frac{2\gamma}{\alpha+\gamma} \frac{(\alpha ux)^{n-1}}{E_0 \Gamma(n)} \alpha x e^{-x} \quad (24)$$

Eq. (24) is strictly valid only for $\alpha ux \gg 1$. A simple trick will be used to obtain a reasonable expression which will be used for all x , and u small enough so that the cross-section assumptions are valid. Eq. (24) is very similar to the expression for the flux according to the straight-ahead approximation, for large ux . Eq. (24) appears then as the first term in the asymptotic expansion of the confluent hypergeometric function. As a plausible guess, the following expression will then be used:

$$\bar{\psi}(x, u) = \frac{n}{E_0} \frac{2\gamma}{\alpha+\gamma} (\alpha x) F(1-n, 2, -\alpha ux) e^{-x} \quad (25)$$

~~SECRET~~

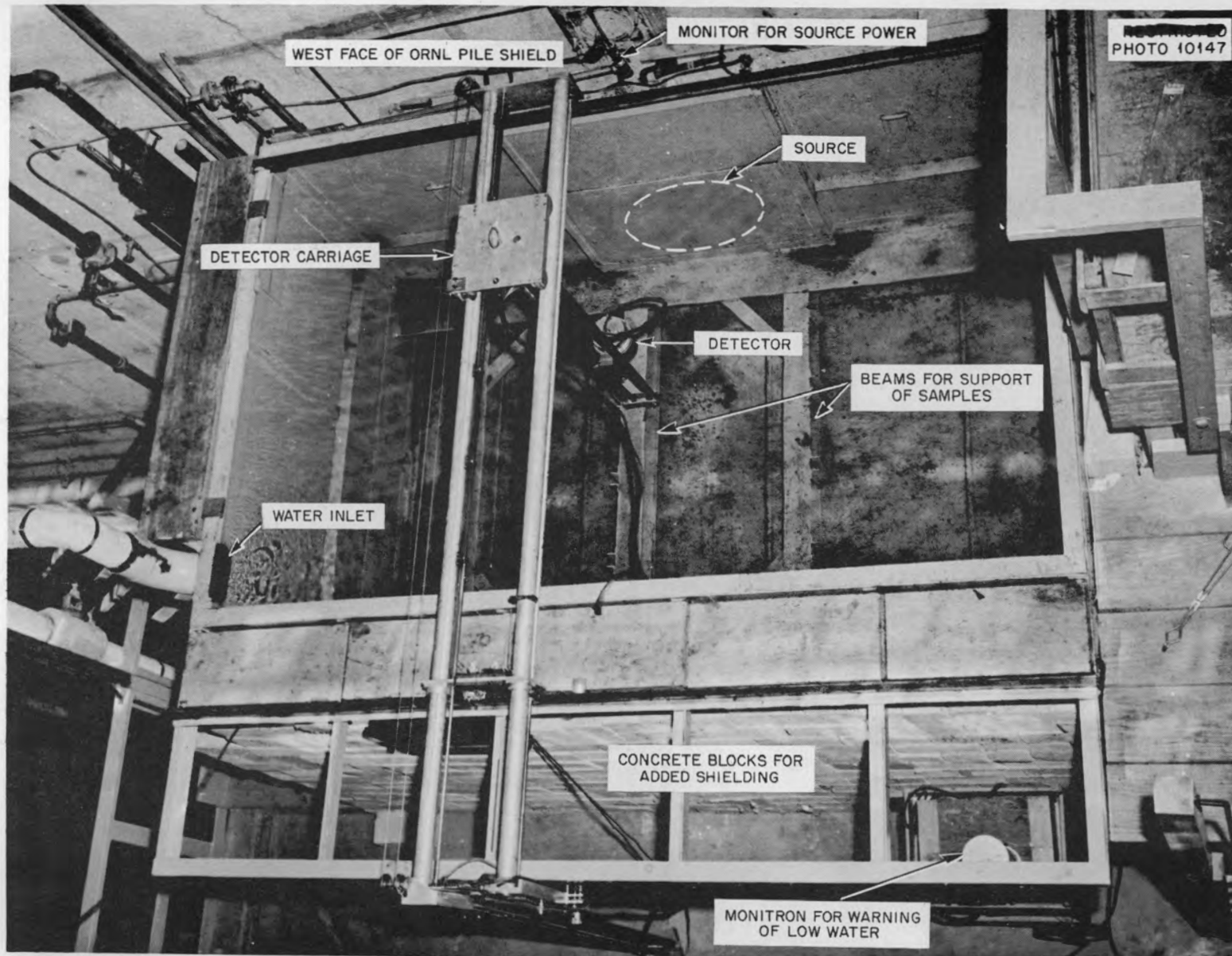
Eq. (25) has the property that for large u it has the correct form (24), and for large d (straight-ahead case) it is good everywhere.

The assumption will be made that neutron dose is proportional to flux for $E > 1$ MEV and is zero for $E < 1$ MEV. Eq. (25) does not include the uncollided contribution, which is easily added. When Eq. (25) is written as a function of energy and appropriate values of d , β , γ , and n are introduced, energies well below E_0 seem to be unimportant for the dosage rate, so that the rather shaky approximations made for large u may not be serious.

The curves of Fig. 11 were obtained by calculating:

$$B(z, E_0) = 1 + \int_1^{E_0} du \frac{dE}{du} \bar{\psi}(\chi, u)$$

The energy E_0 was then set equal to the dominant energy in the uncollided flux at distance z , to obtain $B(z)$.¹⁷



50

Fig. 1 View of Lid Tank from Above.

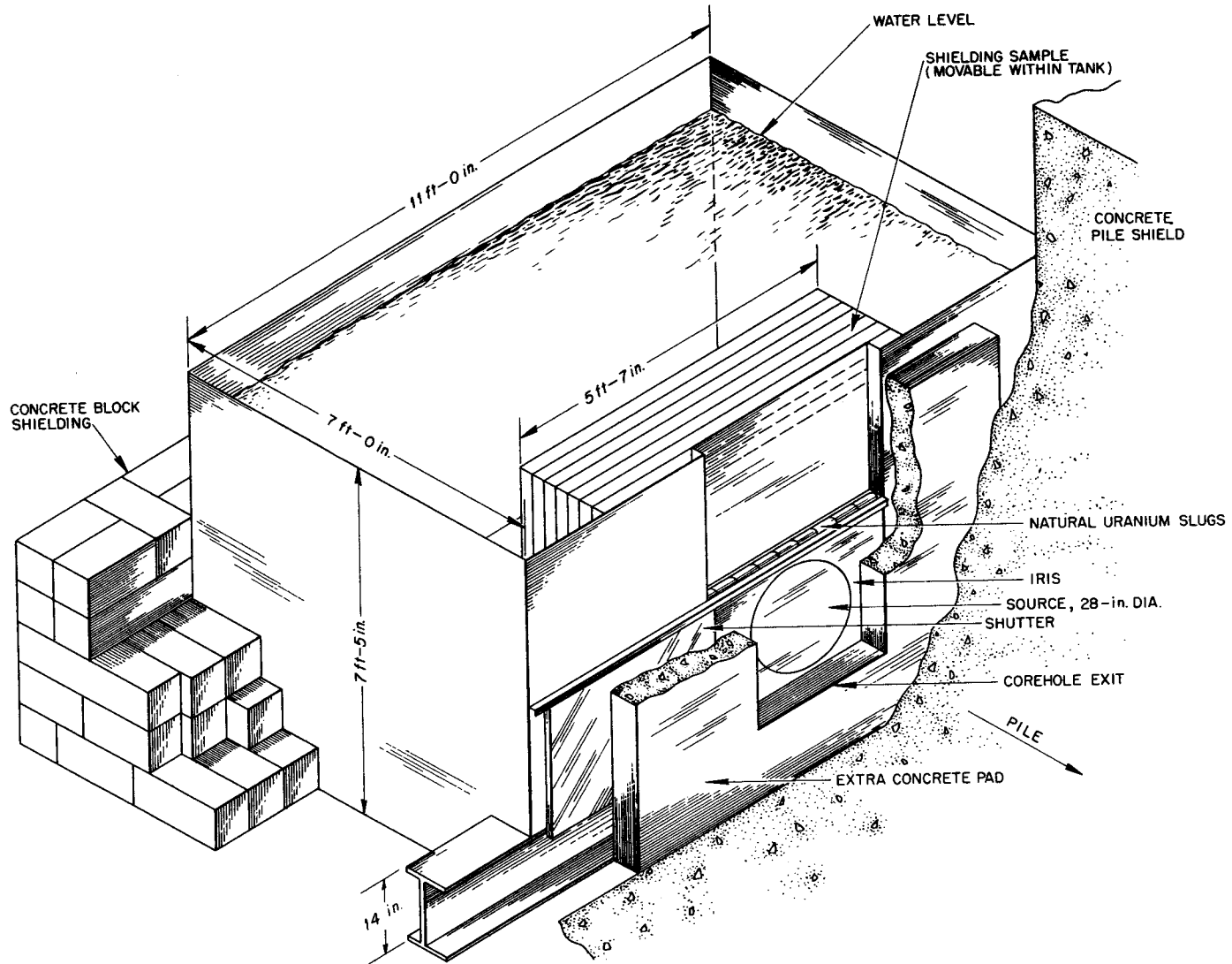


Fig. 2 Isometric View of Lid Tank.

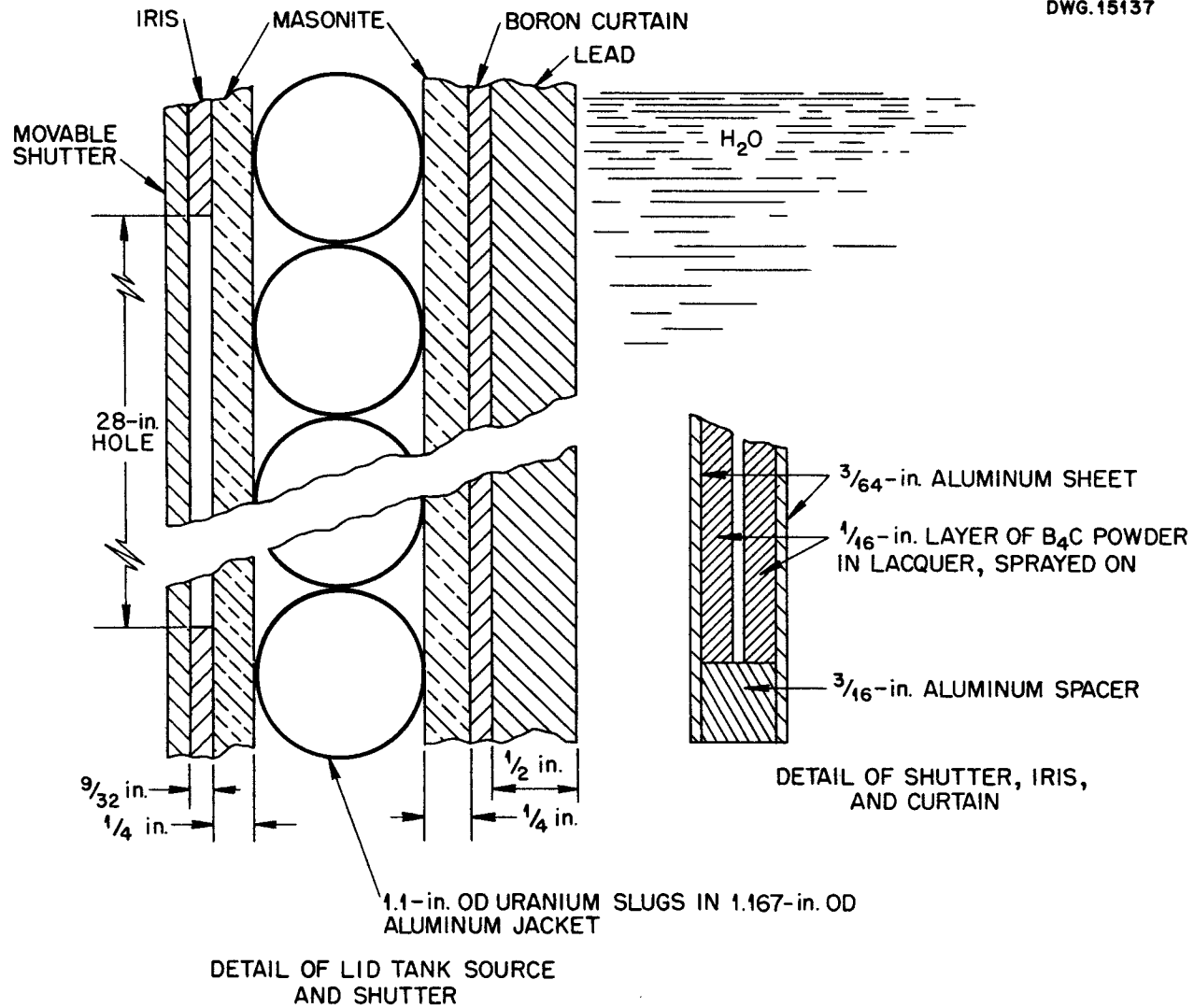


Fig.3 Geometry of Lid Tank Source and Shutter.